2011-07-13

Stability for Traveling Waves

Joshua W. Lytle
Brigham Young University - Provo

Stability for Traveling Waves

Joshua Lytle

A thesis submitted to the faculty of
Brigham Young University
in partial fulfillment of the requirements for the degree of

Master of Science

Jeffrey Humpherys, Chair
John Dallon
Scott Glasgow

Department of Mathematics

Brigham Young University

August 2011

Abstract

Stability for Traveling Waves

Joshua Lytle

Department of Mathematics

Master of Science

In this work we present some of the general theory of shock waves and their stability properties. We examine the concepts of nonlinear stability and spectral stability, noting that for certain classes of equations the study of nonlinear stability is reduced to the analysis of the spectra of the linearized eigenvalue problem. A useful tool in the study of spectral stability is the Evans function, an analytic function whose zeros correspond to the eigenvalues of the linearized eigenvalue problem. We discuss techniques for numerical Evans function computation that ensure analyticity, allowing standard winding number arguments and rootfinding methods to be used to locate eigenvalues. The Evans function is then used to study the spectra of the high Lewis number combustion system, tracking eigenvalues in the right-half plane.

Acknowledgments

I would like to express my deep appreciation to my advisor Jeffrey Humpherys for the substantial amount of time he has given me, and for his constant encouragement and vision. His mentoring has been invaluable throughout my education. I would also like to thank Anna Ghazaryan for the invitation to work with her on the high Lewis number combustion system and for helpful communication regarding this problem.

I would like to thank my parents, Wayne and Marianne Lytle, for their support and encouragement through my education. My thanks also goes to my grandparents for their examples and the inspiration they have been.

I would like to thank my committee members, John Dallon and Scott Glasgow, for making themselves available and providing necessary guidance. I also express my thanks to Lonette Stoddard for her aid throughout my time in the graduate program, and to all my professors who have shared their knowledge and enthusiasm for mathematics. I also thank my colleague Blake Barker for his friendship and the assistance he has provided throughout my study of traveling waves.

Contents

1 Introduction **1**

1.1 Traveling waves 2

1.2 Numerical solution of the traveling wave profile 6

1.3 Stability for traveling waves 11

1.4 The Evans function 19

2 Evans function computation **21**

2.1 Compound matrix method 21

2.2 Polar coordinate method 24

2.3 The method of Kato 27

3 Rootfinding **29**

3.1 Method of moments 29

3.2 Computing the moments of f 31

3.3 A bisection method 33

4 Application: high Lewis number **35**

4.1 The combustion model 35

4.2 Numerical solution of the wave profile 36

4.3 Evans function computation 40

4.4 Rootfinding for $D(\lambda)$ 42

List of Figures

1.1 Re-creation in 1995 of John Russel's initial sighting of a soliton on the Union Canal, Edinburgh. Thanks to Heriot-Watt University, Scotland. 1

1.2 Wave profiles for Burgers equation. 5

1.3 Wave profiles for Burgers equation in state space. 5

1.4 The wave profile for Burgers equation, $\nu = 1$. 9

1.5 The wave profile for Slemrod's capillarity model; $d = 2$. 11

1.6 The wave profile for Slemrod's capillarity model; $d = 60$. 12

3.1 Example of a winding number calculation. 34

4.1 Wave profiles for the high Lewis number combustion system. 40

4.2 Eigenvalues crossing the imaginary axis. 43

4.3 Real part of the eigenvalues. 43

4.4 Imaginary part of the eigenvalues. 44

Chapter 1. Introduction

In this work we discuss traveling waves and their stability properties. A traveling wave is a solution to the evolution equation

$$u_t = f(u, u_x, u_{xx}, \ldots) \tag{1.1}$$

that takes the form $u(x,t) = \hat{u}(x - st)$, where s is the speed of the traveling wave.

Traveling waves occur frequently in nature, in a variety of settings. Interesting problems can be found in fluid flow, gas dynamics, combustion, and population dynamics, to name a few. A classic example of a traveling wave in fluid dynamics is a soliton, a phenomenon discovered by John Russell in 1834 in connection with his work on canal boats. He noted that when a canal boat suddenly stopped moving, a water wave in the form of a pulse continued down the canal with a constant speed, preserving its form.

Figure 1.1: Re-creation in 1995 of John Russel's initial sighting of a soliton on the Union Canal, Edinburgh.

A traveling wave solution $\hat{u}$ of (1.1) may reflect a phenomena that persists. Alternately, the solution may only exist as a transition between states and consequently be observed only infrequently if at all. Mathematically, a traveling wave solution is said to be stable if small perturbations/disturbances of the wave do not alter its form as it continues to evolve. In cases where stability of the physical phenomenon is well known, verification of mathematical stability is an important way of testing the mathematical model.

Stability of a traveling wave may be studied by analyzing the spectrum of the operator linearized about the traveling wave. Indeed, it has been shown by Zumbrun and collaborators [32, 14, 26, 25] that for certain subclasses of (1.1) spectral stability of the linearized operator implies nonlinear stability.

To study spectral stability we introduce the Evans function, a function whose zeros correspond to eigenvalues of the linearized operator. The Evans function is analytic in the right-half plane, allowing us to use standard rootfinding techniques to locate eigenvalues. Energy estimates are often used to find a bounded subset of the right-half plane containing the relevant eigenvalues. A winding number of zero for a contour about the bounded region indicates spectral stability. For those systems that do become spectrally unstable in some parameter regime, we would like to know exactly when and how the instability occurs. We can do this by creating bifurcation diagrams of eigenvalues as they cross into the right-half plane.

1.1 Traveling waves

Consider the class of evolution equations

$$u_t + f(u)_x - \left(B(u)u_x\right)_x + \left(C(u)u_{xx}\right)_x + Q(u) = 0 \tag{1.2}$$

where $x \in \mathbb{R}, u, f \in \mathbb{R}^n$, and $B, C, Q \in \mathbb{R}^{n\times n}$ are sufficiently smooth. The function $f(u)_x$ is the flux or convection/advection of u, $(B(u)u_x)_x$ the diffusion of u, $(C(u)u_{xx})_x$ the dispersion term, and $Q(u)$ the reaction term.

Substituting the ansatz $u(x,t) = \hat{u}(x-st)$ into (1.2) shows that a traveling wave solution is a solution of

$$(f'(u) - s)\, u' - (B(u)u')' + (C(u)u'')' + Q(u) = 0 \tag{1.3}$$

with the necessary boundary conditions. Equivalently, we may view a traveling wave solution as a stationary solution of (1.2) in the moving frame $(x - st, t)$; that is, we transform (1.2) by $(x,t) \to (x - st, t)$ to obtain the equation

$$u_t = \mathcal{F}(u) = -(f'(u) - s)\, u_x + (B(u)u_x)_x - (C(u)u_{xx})_x - Q(u), \tag{1.4}$$

of which $\hat{u}$ is a stationary solution.

We look for traveling wave solutions with asymptotic boundary conditions; that is, solutions $\hat{u}$ satisfying $\hat{u}(\pm\infty) = u_\pm$, $\hat{u}^{(n)}(\pm\infty) = 0$ for $n \geq 1$. For a nontrivial traveling wave $\hat{u}$, if $u_+ = u_-$ the wave is called a pulse; otherwise it is called a wave front or a shock layer, and is said to have amplitude $|u_+ - u_-|$. Because our traveling wave solutions have asymptotically constant end-states, showing existence of a traveling wave is equivalent to finding an orbit connecting the two end-states in some appropriate phase space.

Example 1.1. A prototypical nonlinear advection diffusion equation is Burgers equation, given by

$$u_t + uu_x = \nu u_{xx}, \quad \nu > 0. \tag{1.5}$$

Using dimensional analysis we find that the scaling $(x,t) \to (\frac{x}{\nu}, \frac{t}{\nu})$ removes dependence on

ν, so we can assume $\nu = 1$.

Transforming to the moving frame $(x,t) \to (x - st, t)$, our equation becomes

$$u_t - su_x + uu_x = u_{xx}. \tag{1.6}$$

In this setting a traveling wave solution $\hat{u}$ is a steady-state solution, satisfying $\hat{u}_t = 0$. Thus our profile ode is

$$-su' + \left(\frac{u^2}{2}\right)' = u''. \tag{1.7}$$

By integrating from $-\infty$ to x, we obtain

$$-s(u - u_-) + \frac{u^2 - u_-^2}{2} = u'. \tag{1.8}$$

As $x \to \infty$ we find that

$$-s(u_+ - u_-) + \frac{u_+^2 - u_-^2}{2} = 0,$$

so that the Rankine-Hugoniot condition is $s = \frac{u_+ + u_-}{2}$.

From (1.8) $\hat{u}$ may be solved analytically, obtaining

$$\{\hat{u}(x - st + \delta)\}_{\delta \in \mathbb{R}} = \left\{ s - a \tanh\left(\frac{a(x - st + \delta)}{2}\right) \right\}_{\delta \in \mathbb{R}}, \quad a = \frac{u_- - u_+}{2},$$

as a manifold of solutions to (1.6). See Figures 1.2 and 1.3.

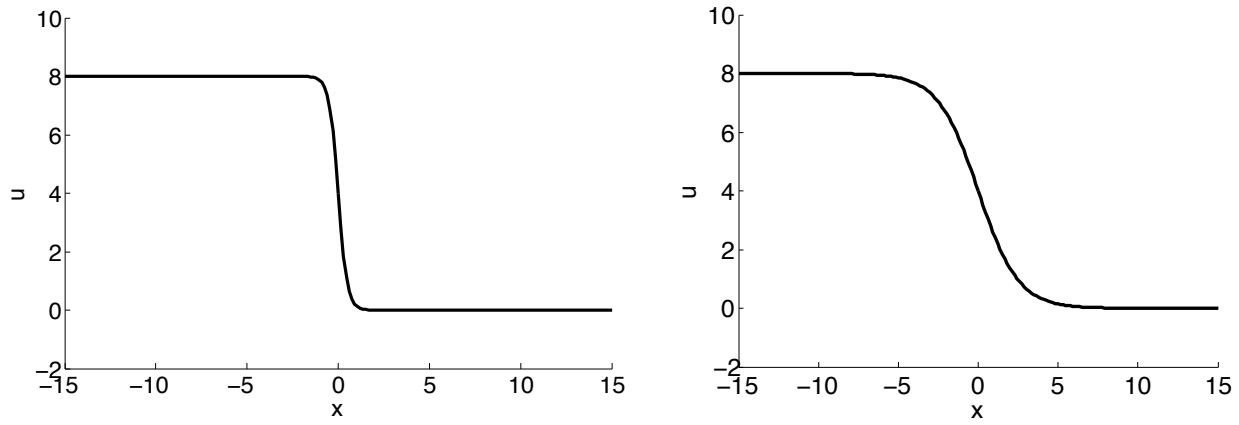

Figure 1.2: Wave profiles for Burgers equation with end-states $u_- = 8$ and $u_+ = 0$. On the left is the solution corresponding to $\nu = 1$; on the right is the solution for $\nu = 5$.

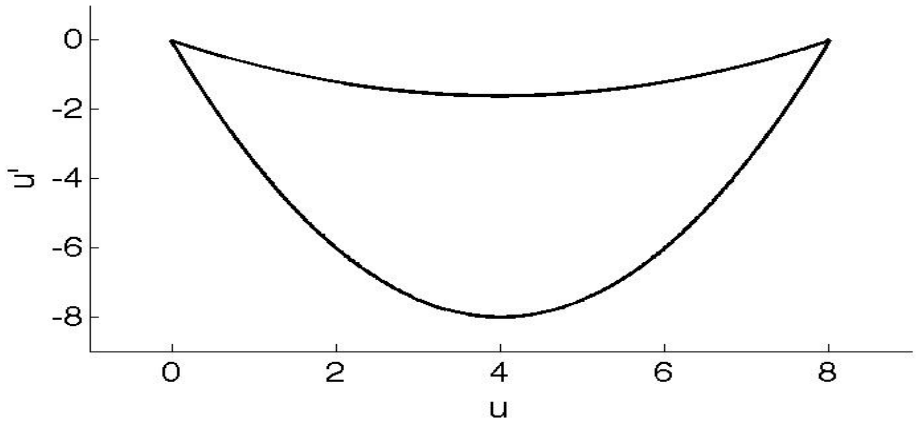

Figure 1.3: Wave profiles for Burgers equation graphed in state space. The end-states $u_- = 8$ and $u_+ = 0$ correspond to rest points. The lower curve corresponds to the profile for $\nu = 1$, with the upper curve corresponding to $\nu = 5$.

1.2 Numerical solution of the traveling wave profile

Consider an asymptotically constant traveling wave solution $u(x,t) = \hat{u}(x-st)$ of (1.1). A traveling wave $\hat{u}$ must be a solution of the following two-point boundary value problem, defined on an infinite domain:

$$\begin{aligned} -su_x &= f(u, u_x, u_{xx}, \ldots), \\ u(\pm\infty) &= u_\pm, \\ u^{(n)}(\pm\infty) &= 0, \quad n \geq 1. \end{aligned} \tag{1.9}$$

A solution of (1.9) corresponds to a connecting orbit between equilibrium points in phase space, with fronts and pulses corresponding to heteroclinic and homoclinic orbits, respectively. Various mathematical tools, including Lyapunov functions, asymptotic ode methods, and topological methods, may be used to determine existence of solutions. Here we give a general description of their numerical solution. Wave profiles in this work have been numerically calculated in Matlab with the aid of **bvp6c**, a function employing sixth-order collocation; see [12].

Numerically solving for the wave profile is often a very difficult problem. For example, note the infinite domain $(-\infty, \infty)$. Since the domain of a traveling wave is the entire real line, and computers cannot solve on an infinite domain, we must numerically solve on a finite domain $[-L, L]$ where L is large enough to capture the behavior of the traveling wave. Likewise, if L is too large other numerical problems can occur. We note that even when solving a particular system, as parameters vary the traveling wave may exhibit very different properties, necessitating careful inspection of the numerical domain for various parameter regimes.

Since our boundary value problem is autonomous, a connecting orbit between two equilibrium points is invariant in x, and thus corresponds to a 1-dimensional manifold of solutions $\{\hat{u}(x+\delta)\}_{\delta\in\mathbb{R}}$. We refer to this as the translational invariance of the traveling wave. Numer-

ically, care must be taken to appropriately specify a particular solution $\hat{u}(x)$.

We begin by writing (1.9) as a first-order system

$$\begin{aligned} u' &= f(u),\ u \in \mathbb{R}^n, \\ u(\pm\infty) &= u_\pm. \end{aligned} \tag{1.10}$$

Let X_S^-, X_U^- be the stable/unstable eigenspaces of $df(u_-)$, X_S^+, X_U^+ the stable/unstable eigenspaces of $df(u_+)$, and $\Pi_S^-, \Pi_U^-, \Pi_S^+, \Pi_U^+$ their corresponding eigenprojections. As $x \to -\infty$ a traveling wave solution $\hat{u}$ must approach u_- along the unstable manifold of u_-. Similarly, as $x \to +\infty$ $\hat{u}$ must approach u_+ along the stable manifold of u_+. In the numerical solver, these (projective) conditions become

$$\Pi_S^-(u(-L) - u_-) = 0,\ \ \Pi_U^+(u(+L) - u_+) = 0,$$

requiring the solution $\hat{u}$ to approach u_- orthogonal to the stable manifold of u_-, and to approach u_+ orthogonal to the unstable manifold of u_+.

Since an orbit in phase space corresponds to a manifold of solutions $\{\hat{u}(x+\delta)\}_{\delta\in\mathbb{R}}$, we give the solver a phase condition $l \cdot u(0) = \alpha$ to determine a specific solution $\hat{u}$. To avoid solving the boundary value problem with a condition in the middle of the domain $[-L, L]$, we double the dimension of the system to $2n$ and add n matching conditions. This allows us to solve for both halves of the profile on the domain $[-L, 0]$.

Numerically solving for the wave profile is often very difficult. There may appear to be too many boundary conditions to enforce. Sometimes this may be handled by adding constant variables to the bvp. For example, when the speed of the wave is not known, adding $s' = 0$ to the system of odes may be necessary. We note that often the projective conditions depend on the wave speed, and so must be updated continuously in the numerical solver.

A boundary value problem also requires an initial guess for the profile. For simple profiles

a guess using the tanh function may be sufficient. In general, however, as parameters vary the solution $\hat{u}(x)$ becomes more complex and difficult to solve, and a decent initial guess becomes harder to obtain. In this case continuation becomes a very useful tool: to obtain wave profiles across some range of parameters, cross the parameter regime stepwise, using a solution at one step as an initial guess for the next.

Example 1.2. Recall equation (1.7), of which the wave profile for Burgers equation is a solution:

$$-su' + uu' = u''.$$

We begin by writing (1.7) as a first order system $y' = f(y)$ where $y_1 = u, y_2 = u'$:

$$\begin{bmatrix} y_1 \\ y_2 \end{bmatrix}' = \begin{bmatrix} y_2 \\ y_2(y_1 - s) \end{bmatrix}.$$

This system has projective conditions $y_1(-L) = u_-$, $y_1(L) = u_+$.

To solve for the full profile on $[-L, 0]$, we let $z(x) = y(-x)$. We then double the dimension of our system to get

$$\begin{bmatrix} y_1 \\ y_2 \\ z_1 \\ z_2 \end{bmatrix}' = \begin{bmatrix} y_2 \\ y_2(y_1 - s) \\ -z_2 \\ z_2(s - z_1) \end{bmatrix},$$

with corresponding projective conditions

$$y_1(-L) = u_-, \;\; z_1(-L) = u_+,$$

a phase condition

$$y_1(0) = \frac{u_- + u_+}{2},$$

and matching condition

$$z_1(0) = y_1(0).$$

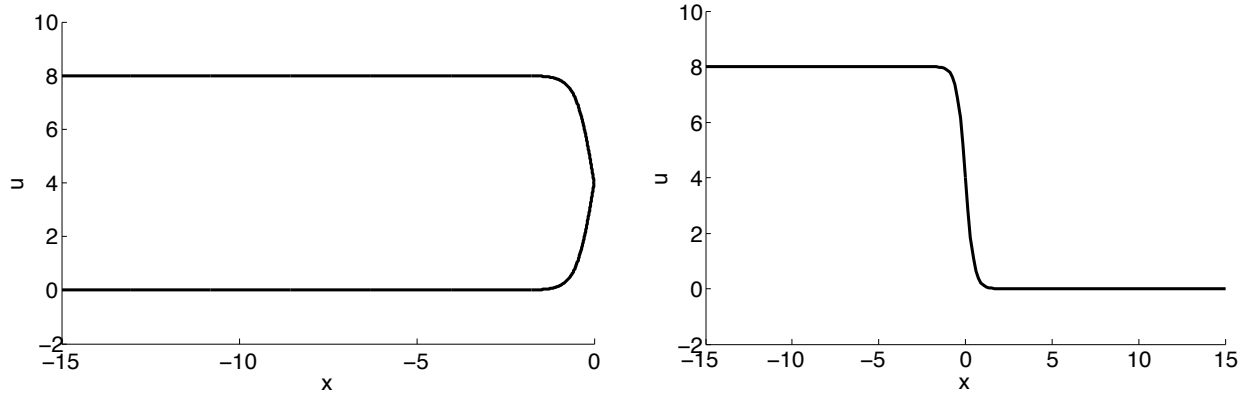

Figure 1.4: The wave profile for Burgers equation solved numerically on $[-15, 0]$. After solving numerically, the lower solution $z(x)$ is flipped onto $[0, 15]$.

Example 1.3. Consider Slemrod's model for 1-dimensional isentropic gas dynamics with capillarity:

$$\begin{aligned} v_t - u_x &= 0, \\ u_t + p(v)_x &= \left(\frac{u_x}{v}\right)_x - dv_{xxx}. \end{aligned} \tag{1.11}$$

Here v is the specific volume, u is velocity in Lagrangian coordinates, $p(v)$ is the pressure law for an ideal gas (so $p'(v) < 0$ and $p''(v) > 0$), and $d \geq 0$ is capillarity strength.

We look for a traveling wave solution $(u, v)(x, t) = (\hat{u}, \hat{v})(x - st)$ with asymptotically constant end states $(\hat{u}, \hat{v})(\pm\infty) = (u_\pm, v_\pm)$. By translating to the moving frame $(x, t) \to (x - st, t)$ our system becomes

$$\begin{aligned} v_t - sv_x - u_x &= 0, \\ u_t - su_x + p(v)_x &= \left(\frac{u_x}{v}\right)_x - dv_{xxx}. \end{aligned} \tag{1.12}$$

By rescaling $(x,t,u) \to (-sx, s^2t, -u/s)$ we obtain

$$\begin{aligned} v_t + v_x - u_x &= 0, \\ u_t + u_x + ap(v)_x &= \left(\frac{u_x}{v}\right)_x - dv_{xxx}, \end{aligned} \tag{1.13}$$

where $a = 1/s^2$. This simplifies to a single ode for v:

$$v' + ap(v)' \;=\; \left(\frac{v'}{v}\right)' - dv'''. \tag{1.14}$$

Integrating from $-\infty$ to x gives

$$v - v_- + a(p(v) - p(v_-)) = \frac{v'}{v} - dv'' \tag{1.15}$$

as our profile ode. We then find a by letting $x \to \infty$, obtaining the Rankine-Hugoniot condition

$$a = -\frac{v_+ - v_-}{p(v_+) - p(v_-)}.$$

Without loss of generality we can assume $0 < v_+ < v_-$. Also, after rescaling we may assume that $v_- = 1$; see [4, 15, 16]. We will assume a gas law of the form $p(v) = v^{-\gamma}, \gamma \geq 1$.

Let $y_1 = v, y_2 = v'$. Then written as a first order system $y' = f(y)$ we have

$$\begin{bmatrix} y_1 \\ y_2 \end{bmatrix}' \;=\; \begin{bmatrix} y_2 \\ \frac{1}{d}[y_2/y_1 + (1-y_1) + a(1-y_1^{-\gamma})] \end{bmatrix}. \tag{1.16}$$

Checking $df(v_-)$ and $df(v_+)$ we find one projective condition at $x = +\infty$.

To solve for the full profile on $[-L, 0]$ we let $z(x) = y(-x)$, allowing us to solve the system

$$\begin{bmatrix} y \\ z \end{bmatrix}' \;=\; \begin{bmatrix} f(y) \\ -f(z) \end{bmatrix} \tag{1.17}$$

with one projective condition, two matching conditions

$$y_1(0) = z_1(0), \tag{1.18}$$

$$y_2(0) = z_2(0), \tag{1.19}$$

and one phase condition

$$y_1(0) = \frac{v_- + v_+}{2}.$$

As capillarity strength d increases, the wave becomes highly oscillatory; see Figures 1.5 and 1.6. This system is a good example of when continuation could be helpful.

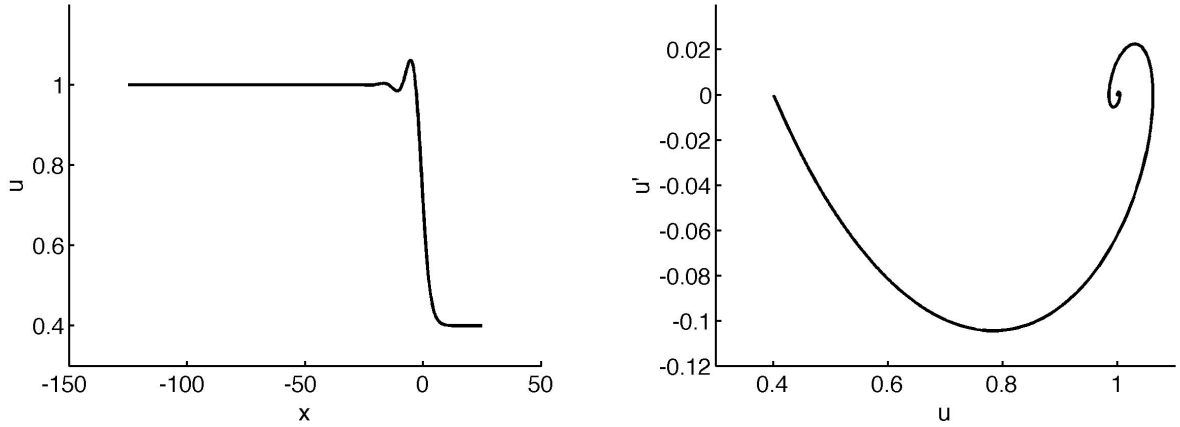

Figure 1.5: The wave profile for Slemrod's capillarity model, also shown in state space. Here capillarity strength is $d = 2$.

1.3 Stability for traveling waves

First we note that a traveling wave solution $\hat{u}$ of (1.2) is a stationary solution of (1.4), that is, $\mathcal{F}(\hat{u}) = 0$. Let X be a suitable Banach space, and $\mathcal{A} \subset X$ an admissible set of perturbations.

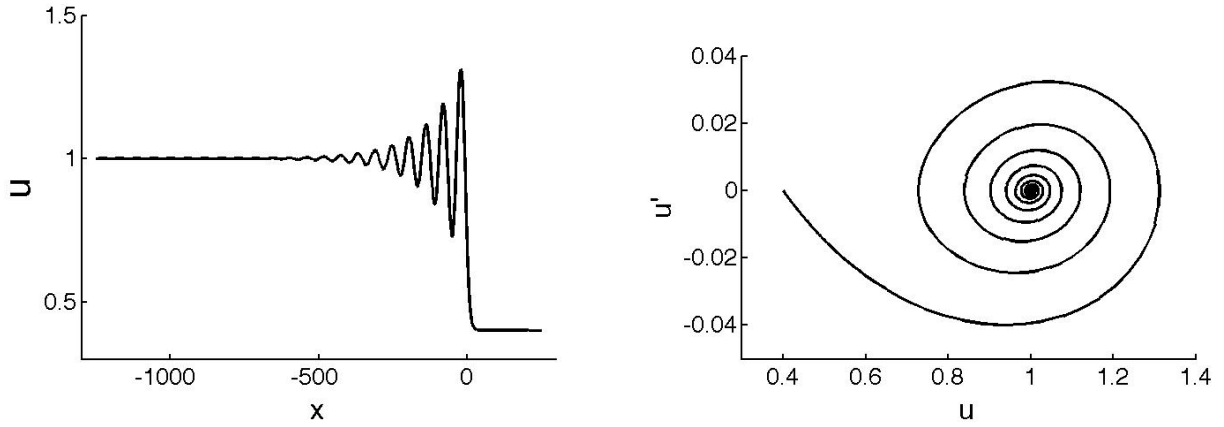

Figure 1.6: The wave profile for Slemrod's capillarity model, with capillarity strength $d = 60$.

The Cauchy problem we wish to consider for (1.4) is to find solutions $u(x,t)$ of

$$\begin{aligned} u_t &= \mathcal{F}(u), \\ u(x,0) &= \hat{u}(x) + v(x,0),\ v(x,0) \in \mathcal{A}, \end{aligned} \tag{1.20}$$

for perturbations $v \in \mathcal{A}$.

A fundamental question concerning traveling wave solutions is the following: Will the perturbation $u(x)$ of a traveling wave solution $\hat{u}(x)$ converge to (some translate of) $\hat{u}$ as $t \to \infty$, or will it evolve into something else? This question motivates the following definition:

Definition 1.4. We say that a stationary solution $\hat{u}$ of (1.4) is *asymptotically orbitally stable* with respect to the set of perturbations $\mathcal{A}$ if $u(\cdot,t) \to \hat{u}(x+\delta)$ for some δ as $t \to \infty$ whenever $u(x,0) - \hat{u}(x) = v(x,0) \in \mathcal{A}$. We may use interchangeably the terms *asymptotic orbital stability and nonlinear stability.*

In general spectral stability of the wave profile is a weaker condition than nonlinear stability, however for certain classes of equations spectral stability has been shown to imply nonlinear stability; see [32, 14, 26, 25].

To obtain the eigenvalue problem, we linearize

$$u_t = -(f'(u) - s)u_x + (B(u)u_x)_x - (C(u)u_{xx})_x - Q(u)$$

about the stationary solution $\hat{u}$, getting

$$\lambda v \quad = \quad Lv := -(A(\hat{u})v)_x + (B(\hat{u})v_x)_x - (C(\hat{u})v_{xx})_x - Q'(\hat{u})v \tag{1.21}$$

where $A(\hat{u})v = (f'(\hat{u} - B'(\hat{u})\hat{u}_x + C'(\hat{u})\hat{u}_{xx} - s)v$.

Definition 1.5. For the linear operator L (1.21), the

(i) spectrum $\sigma(L)$ of L is the set of all $\lambda \in \mathbb{C}$ where $L - \lambda I$ is not invertible.

(ii) point spectrum $\sigma_p(L)$ of L is the set of all isolated eigenvalues of L with finite multiplicity.

(iii) essential spectrum $\sigma_e(L)$ of L is the spectrum of L minus the point spectrum: $\sigma(L)\backslash\sigma_p(L)$.

Definition 1.6. The operator L in 1.21 is spectrally stable if its spectrum does not extend into the closed deleted right half plane $\sum_+ = \{\lambda \in \mathbb{C}\backslash\{0\} : \mathrm{Re}(\lambda) \geq 0\}$.

A formal argument that spectral stability may be used to determine nonlinear stability goes as follows: We linearize (1.4) about $\hat{u}$, obtaining

$$u_t = F(u) = F(\hat{u}) + dF(\hat{u})v + Q(v),$$

where $Q(v) = \mathcal{O}(|v|^2)$. Any initial state u can be written as $u = \hat{u} + v$, where v is a

perturbation of $\hat{u}$. Then we obtain

$$\begin{aligned}
(\hat{u}+v)_t &= F(\hat{u}) + dF(\hat{u})v + Q(v),\\
v_t &= dF(\hat{u})v + Q(v),\\
&= Lv + Q(v),\\
v_t - Lv &= Q,\\
e^{-Lt}v_t - e^{-Lt}Lv &= e^{-Lt}Q,\\
\int_0^t \left(e^{-Lt}v(s)\right)' ds &= \int_0^t e^{-Ls}Q(s)ds,\\
e^{-Lt}v(t) - v_0 &= \int_0^t e^{-Ls}Q(s)ds,\\
v(t) &= e^{Lt}v_0 + e^{Lt}\int_0^t e^{-Ls}Q(s)ds,\\
&= e^{Lt}v_0 + \int_0^t e^{L(t-s)}Q(s)ds.
\end{aligned}$$

Since v is small and $Q \sim \mathcal{O}(v^2)$, $\int_0^t e^{L(t-s)}Q(s)ds$ is negligible and $v \approx e^{Lt}v_0$.

We note that 0 is always an eigenvalue of L, and is associated with the translational invariance of the traveling wave. Thus the linearized operator L always has a nontrivial spectrum.

Lemma 1.7 (Sattinger [27])**.** *The derivative of $\hat{u}$ is an eigenfunction of L with eigenvalue 0.*

Proof. By translational invariance of the traveling wave, $\mathcal{F}(\hat{u}(x+\delta)) = 0$ for each $\delta \in \mathbb{R}$. Then $\frac{d}{d\delta}\left(\mathcal{F}(\hat{u}(x+\delta))\right|_{\delta=0} = d\mathcal{F}(\hat{u})\hat{u}' = 0$, so $\hat{u}'$ is an eigenvector of $L = d\mathcal{F}(\hat{u})$ with eigenvalue 0. □

To prove spectral stability of L it is necessary to show that the essential spectrum and the point spectrum of L do not intersect the closed deleted right-half plane $\sum_+$. In the next two sections we will deal with the essential and point spectrums separately, giving some of

the most pertinent results.

1.3.1 Essential spectrum. The following result is very useful in dealing with the essential spectrum of L:

Theorem 1.8 (Henry [13])**.** *The essential spectrum of L in (1.21) is sharply bounded to the left of*

$$\sigma_e(L_+) \cup \sigma_e(L_-), \tag{1.22}$$

where $L_\pm$ correspond to the operators obtained by linearizing about the constant solutions $\hat{u} = u_\pm$, respectively.

Proof. We note that linearization about $u_\pm$ yields

$$v_t = L_\pm v = -A_\pm v_x + B_\pm v_{xx} - C_\pm v_{xxx} - D_\pm v, \tag{1.23}$$

where $A_\pm = A(u_\pm), \ldots, D_\pm = D(u_\pm)$ are constant matrices. Then $\sigma(L_\pm) = \sigma_e(L_\pm)$ since constant coefficient linear operators do not have a point spectrum. We use the Fourier transform to make a formal argument concerning $\sigma_e(L_\pm)$.

Now

$$\widehat{(L - \lambda I)}^{-1} v = (-i\xi A_\pm - \xi^2 B_\pm + i\xi^3 C_\pm - D_\pm - \lambda I)^{-1} v \tag{1.24}$$

where $\xi \in \mathbb{R}$. We note that invertibility of $L - \lambda I$ is lost whenever $-i\xi A_\pm - \xi^2 B_\pm + i\xi^3 C_\pm - D_\pm - \lambda I$ is singular, so that

$$\lambda \in \sigma(L_\pm) \quad \text{iff} \quad \lambda \in \sigma(-i\xi A_\pm - \xi^2 B_\pm + i\xi^3 C_\pm - D_\pm) \tag{1.25}$$

for some $\xi \in \mathbb{R}$. Thus we have $2n$ curves $\lambda_j^\pm$ corresponding to the eigenvalues of the right-

hand side, giving

$$\sigma_e(L_+) \cup \sigma_e(L_-) = \bigcup_j \lambda_j^+(\xi) \cup \bigcup_j \lambda_j^-(\xi). \tag{1.26}$$

Thus, we may use the structure of $A_\pm, B_\pm, C_\pm$, and $D_\pm$ to obtain sharp bounds on the essential spectrum of L. This gives us a way to see if $\sigma_e(L)$ intersects the closed right half plane $\sum_+$. □

1.3.2 Point spectrum. The problem of obtaining bounds on the point spectrum of L is generally much harder than dealing with the essential spectrum. Energy estimates have proven to be a useful tool in many instances, although their application is often not obvious or intuitive.

One of the difficulties associated with obtaining uniform bounds stems from the presence of 0 in the point spectrum of L. For the reactionless equation (1.21) ($Q(u) = 0$), the eigenvalue problem may instead be viewed in integrated coordinates. Specifically, by integrating both sides of

$$\lambda v \;=\; Lv = -(A(\hat{u})v)_x + (B(\hat{u})v_x)_x - (C(\hat{u})v_{xx})_x \tag{1.27}$$

from $-\infty$ to x, and substituting $w = \int_{-\infty}^{x} v$, we obtain the integrated operator

$$\lambda w \;=\; \mathcal{L}w := -A(\hat{u})w' + B(\hat{u})w'' - C(\hat{u})w'''. \tag{1.28}$$

The following result is very useful.

Lemma 1.9. *The point spectrum of $\mathcal{L}$ is the same as L, excluding $\lambda = 0$.*

Proof. Suppose $\lambda v = Lv$ with $\lambda \neq 0$. Integrating both sides from $-\infty$ to x and substituting

$w = \int_{-\infty}^{x} v$ yields $\lambda w = \mathcal{L}w$. Since

$$\lambda w(+\infty) = -\int_{-\infty}^{\infty} (Av)' + \int_{-\infty}^{\infty} (Bv')' - \int_{-\infty}^{\infty} (Cv'')' = 0,$$

we note that $w^{(n)}$ decays to 0 for $n = 0, 1, \ldots$. Thus w is an admissible eigenvector and $\sigma(L)\backslash\{0\} \subset \sigma(\mathcal{L})$.

Now suppose $\lambda w = \mathcal{L}w$, $\lambda \neq 0$. Differentiating yields

$$\lambda w' = -(Aw')' + (Bw'')' - (Cw''')',$$

making w' an eigenvalue of L. Thus $\sigma_p(\mathcal{L})\backslash\{0\} = \sigma_p(L)\backslash\{0\}$. □

Example 1.10. Consider again Burgers equation

$$u_t + uu_x = u_{xx}.$$

A traveling wave solution $\hat{u}$ of Burgers equation is a steady state solution of

$$u_t - su_x + uu_x = u_{xx}. \tag{1.29}$$

We let $u = \hat{u} + v$. Substituting into (1.29), we obtain

$$\hat{u}_t + v_t - s\hat{u}_x - sv_x + \hat{u}\hat{u}_x + v\hat{u}_x + \hat{u}v_x + vv_x = \hat{u}_{xx} + v_{xx}.$$

Since vv_x is considered to be small and $\hat{u}_t - s\hat{u}_x + \hat{u}\hat{u}_x = \hat{u}_{xx}$, we get

$$v_t - sv_x + \hat{u}_x v + \hat{u}v_x = v_{xx}.$$

We can write this as $v_t = Lv$ where L is the differential operator given by

$$\begin{aligned} Lv = &\quad sv_x - \hat{u}_x v - \hat{u}v_x + v_{xx}, \\ = &\qquad sv_x - (\hat{u}v)_x + v_{xx}. \end{aligned} \tag{1.30}$$

Integrating both sides of 1.30 from $-\infty$ to x and substituting $w = \int_{-\infty}^{x} v$ yields

$$\lambda w = (s - \hat{u})w' + w'' \tag{1.31}$$

as our eigenvalue problem in integrated coordinates.

Example 1.11. We will use an energy estimate to show stability for Burgers equation. Multiplying both sides of 1.31 by $\overline{w}$ and integrating over the real line, we obtain

$$\lambda \int_{\mathbb{R}} |w|^2 = \int_{\mathbb{R}} (s - \hat{u})\overline{w}w' + \int_{\mathbb{R}} \overline{w}w''.$$

Integration by parts gives

$$\begin{aligned} \int_{\mathbb{R}} \overline{w}w'' &= \overline{w}w'|_{-\infty}^{\infty} - \int_{\mathbb{R}} |w'|^2, \\ &= -\int_{\mathbb{R}} |w''|^2, \end{aligned} \tag{1.32}$$

so that

$$\lambda \int_{\mathbb{R}} |w|^2 = \int_{\mathbb{R}} (s - \hat{u})\overline{w}w' - \int_{\mathbb{R}} |w'|^2. \tag{1.33}$$

Integrating $(s - \hat{u})\overline{w}w'$ by parts gives

$$\int_{\mathbb{R}} (s - \hat{u})\overline{w}w' = (s - \hat{u})\overline{w}w|_{-\infty}^{\infty} - \int_{\mathbb{R}} (s - \hat{u}\overline{w}'w + \int_{\mathbb{R}} w\overline{w}\hat{u}', \tag{1.34}$$

so that

$$\text{Real}(\lambda)\int_{\mathbb{R}}|w|^2 = 1/2\int_{\mathbb{R}}|w|^2\hat{u}' - \int_{\mathbb{R}}|w'|^2 < 0 \tag{1.35}$$

since $\hat{u}' < 0$. Thus $\text{Real}(\lambda) < 0$.

Example 1.12. Here we find a bound on the essential spectrum of the eigenvalue problem for Burgers,

$$v_t = -((\hat{u} - s)v)_x + v_{xx}.$$

Taking the Fourier transform of the eigenvalue problem linearized about $u_\pm$, we see that the essential spectrum must be to the left of the curves given by

$$\lambda = -i(u_\pm - s)\xi - \xi^2, \tag{1.36}$$

$$= \pm i\frac{u_- - u_+}{2}\xi - \xi^2, \ \ \xi \in \mathbb{R}. \tag{1.37}$$

These curves define a parabola in the left half of the complex plane that touches the origin at $\xi = 0$.

A similar proof can be used to show spectral stability for the general scalar conservation law

$$u_t + f(u)_x = (b(u)u_x)_x;$$

see [18] for further examples of energy estimates.

1.4 The Evans function

Consider again the eigenvalue problem

$$\lambda v = Lv = d\mathcal{F}(\hat{u})v. \tag{1.38}$$

After bounding the essential spectrum of L, we use the Evans function to analyze eigenvalues to the right of the essential spectrum.

We define the Evans function as the Wronskian of decaying solutions of (1.38). The Evans function is analytic to the right of the essential spectrum, with roots corresponding exactly with the eigenvalues of L in both location and multiplicity; see [1] .

We write the eigenvalue problem (1.38) as a first-order system

$$\lambda W' = A(x,\lambda)W, \;\; W \in \mathbb{C}^n, \;\; ' = \frac{\mathrm{d}}{\mathrm{d}x}. \tag{1.39}$$

We note that eigenvalues of (1.38) are values of λ with an associated nontrivial solution W of (1.39), satisfying $W(\pm\infty) = 0$. We also note that $A(x,\lambda)$ is asymptotically constant in x since $\hat{u}$ is. Thus we can consider the constant coefficient matrices $A_\pm(\lambda) = \lim_{x\to\pm\infty} A(x,\lambda)$. An eigenvector W of (1.38) must approach the origin along the unstable manifold $U^-(\lambda)$ of $A_-(\lambda)$, and the stable manifold $S^+(\lambda)$ of $A_+(\lambda)$. We will assume consistent splitting of $A(x,\lambda)$; i.e., the dimensions of $U^-(\lambda)$ and $S^+(\lambda)$ are k and $n-k$, respectively, for some k.

Suppose $r_1^-(\lambda),\ldots,r_k^-(\lambda)$ and $r_{k+1}^+(\lambda),\ldots,r_n^+(\lambda)$ are analytically varying bases for $U^-(\lambda)$ and $S^+(\lambda)$, respectively. Let $W_i^-(\lambda)$ be the solution of 1.39 where $W_i^-(\lambda) \to 0$ along $r_i^-(\lambda)$ as $x \to -\infty$. We define $W_i^+(\lambda)$ similarly. We then define the Evans function by

$$D(\lambda) := \det(W_1^-(\lambda)\ldots W_k^-(\lambda), W_{k+1}^+(\lambda)\ldots W_n^+(\lambda))\big|_{x=0}. \tag{1.40}$$

We note that $D(\lambda) = 0$ iff $W_1^-(\lambda),\ldots,W_k^-(\lambda),W_{k+1}^+(\lambda)\ldots,W_n^+(\lambda)$ are linearly dependent. In this case we have an eigenvector W living on both $U^-(\lambda)$ and $S^+(\lambda)$. We remark that analyticity of $D(\lambda)$ depends on finding analytically varying bases for $U^-(\lambda)$ and $S^+(\lambda)$.

The Evans function is rarely solved analytically, and then only for simple systems; for example, the Evans function for Burgers equation is found analytically in [3]. In practice $D(\lambda)$ is computed numerically by integrating $U^-(\lambda)$ and $S^+(\lambda)$ from $\pm\infty$ to 0.

Chapter 2. Evans function computation

Numerical computation of the Evans function has essentially two basic parts. First, bases for $U^-(\lambda)$ and $S^+(\lambda)$ must be computed. These bases must vary analytically in λ. The second component is the integration of $U^-(\lambda)$ and $S^+(\lambda)$ from $\pm\infty$ to 0. If both parts are done accurately, $D(\lambda)$ will be analytic, allowing us to employ standard winding number arguments and rootfinding techniques to locate and track eigenvalues.

In this chapter we consider several common difficulties associated with the numerical implementation of the Evans function. We will discuss the compound matrix method and the polar coordinate method [17] as solutions to the problem of integration; see [31, 17, 3] for further details. A standard result due to Kato [21] will be given, from which we will find analytically varying eigenprojections.

2.1 Compound matrix method

Consider again the first-order, linear boundary value problem

$$\begin{aligned} W' &= A(x,\lambda)W,\ W \in \mathbb{C}^n,\ ' = \frac{\mathrm{d}}{\mathrm{d}x}, \\ W(\pm\infty) &= 0, \end{aligned} \tag{2.1}$$

whose nontrivial solutions $(\lambda, W(\lambda))$ correspond to eigenpairs of L. In this section we will lift (2.1) into the exterior product space $\wedge^k(\mathbb{C}^n)$.

First we recall that $\wedge^k(\mathbb{C}^n)$ is the space of finite sums of k-forms of elements of $\mathbb{C}^n$, with the k-forms being multilinear and alternating. We note that it is quite easy to obtain a basis for $\wedge^k(\mathbb{C}^n)$: if $\{e_1, \ldots, e_n\}$ is a basis for $\mathbb{C}^n$, then $\{e_{j_1} \wedge \ldots \wedge e_{j_k}, 1 \le j_1 < j_2 < \ldots < j_k \le n\}$ is a basis for $\wedge^k(\mathbb{C}^n)$. Thus $\wedge^k(\mathbb{C}^n)$ is a $\binom{n}{k}$ dimensional space; see [7] for details on this

space.

Given vectors $x_1, \ldots, x_k$ in $\mathbb{C}^n$, if $x_1, \ldots, x_k$ are linearly independent then $x_1 \wedge \ldots \wedge x_k$ becomes a k-form representing the span of $x_1, \ldots, x_k$ as a point in $\wedge^k(\mathbb{C}^n)$. In particular, the k-dimensional unstable eigenspace of $A_-(\lambda)$ becomes a single vector in $\wedge^k(\mathbb{C}^n)$. The lifted problem is given by

$$W' = A^{(k)}W, \;\; W = w_1 \wedge \ldots \wedge w_k \in \mathbb{R}^{\binom{n}{k}}, \tag{2.2}$$

where

$$\begin{aligned} A^{(k)} \circ W &= (Aw_1) \wedge w_2 \wedge \ldots \wedge w_k + \\ &\quad w_1 \wedge (Aw_2) \wedge \ldots \wedge w_k + \ldots \\ &\quad w_1 \wedge w_1 \wedge \ldots \wedge (Aw_k). \end{aligned} \tag{2.3}$$

Let $\{r_j^-\}_{j=1}^k$ and $\{r_j^+\}_{j=k+1}^n$ be the right eigenvectors of $A_-(\lambda)$ and $A_+(\lambda)$ respectively, spanning U^- and S^+. Let $\{\mu_j^-\}_{j=1}^k$ and $\{\mu_j^+\}_{j=k+1}^n$ be their corresponding eigenvalues. Then the unstable manifold $U^-(x)$ of $A_-(\lambda)$ may be represented as a wedge product $U^-(x) = W_1^-(x) \wedge \ldots \wedge W_k^-(x)$, with W_j^- satisfying

$$\begin{aligned} W_j^{-\prime} &= A(x,\lambda)W_j^-, \\ W_j^-(x) &\approx e^{\mu_j^- x} r_j^-, \quad x << 0. \end{aligned} \tag{2.4}$$

Similarly the stable manifold $S^+(x)$ of $A_+(\lambda)$ may be represented as a wedge product $S^+(x) = W_{k+1}^+(x) \wedge \ldots \wedge W_n^+(x)$ in $\wedge^{n-k}(\mathbb{C}^n)$, with W_j^+ satisfying

$$\begin{aligned} W_j^{+\prime} &= A(x,\lambda)W_j^+, \\ W_j^+(x) &\approx e^{\mu_j^+ x} r_j^+, \quad x >> 0. \end{aligned} \tag{2.5}$$

We note the isomorphism

$$U^-(x) \wedge S^+(x) = W_1^-(x) \wedge \ldots \wedge W_k^-(x) \wedge W_{k+1}^+(x) \wedge \ldots \wedge W_n^+(x), \tag{2.6}$$

$$\approx \det\left[W_1^-(x) \ldots W_k^-(x), W_{k+1}^+(x) \ldots W_n^+(x)\right], \tag{2.7}$$

The Evans function is then defined as

$$D(\lambda) = U^-(x) \wedge S^+(x)\big|_{x=0},$$

and is analytic in λ if $\{r_j^{\pm}(\lambda)\}$ vary analytically.

There are several numerical difficulties associated with the Evans function that must be addressed. First we note that the manifolds U^-, S^+ must be found by integrating from $x = \pm\infty$ to $x = 0$. It is numerically difficult to resolve growth on different modes. Numerical (and round-off) error tends to accumulate on the largest growth mode. For example, when $n = 4, k = 2$ suppose there are growth modes $\mu_1^- > \mu_2^- > 0$ at $x = -\infty$. Integrating $W_2^-(x)$ from $-\infty$ to 0, error accumulates so that $W_2^-(x)$ becomes $aW_1^-(x) + bW_2^-(x)$. To obtain accurate results the step size of the integration must decrease, causing computation to slow.

By lifting the eigenvalue problem into the exterior product space $\Lambda^k(\mathbb{C}^n)$, the manifold U^- becomes a k-product $W_1^- \wedge \ldots \wedge W_k^-$, an eigenvector of the lifted problem corresponding to its largest mode. In this way the compound matrix method provides accurate multi-mode resolution.

Lemma 2.1. *Suppose $(\mu_1, r_1), \ldots, (\mu_k, r_k)$ are eigenpairs of A. Then $r_1 \wedge \ldots \wedge r_k$ is an eigenvector of $A^{(k)}$ with eigenvalue $\mu_1 + \ldots + \mu_k$.*

Proof.

$$\begin{aligned} A^{(k)} \circ (r_1 \wedge \ldots \wedge r_k) &= (Ar_1) \wedge r_2 \wedge \ldots \wedge r_k + \\ &\quad r_1 \wedge (Ar_2) \wedge \ldots \wedge r_k + \ldots \\ &\quad r_1 \wedge r_2 \wedge \ldots \wedge (Ar_k), \\ &= (\mu_1 r_1) \wedge \ldots \wedge r_k + \ldots \\ &\quad r_1 \wedge \ldots \wedge (\mu_k r_k), \\ &= (\mu_1 + \ldots + \mu_k) r_1 \wedge r_2 \wedge \ldots \wedge r_k. \end{aligned}$$

□

Corollary 2.2. *Suppose $\mu_1, \ldots, \mu_k$ are the largest eigenvalues of A. Then $\mu_1 + \ldots + \mu_k$ is the largest eigenvalue of $A^{(k)}$.*

2.2 Polar coordinate method

Note that an exterior product $\Lambda \in \Lambda^k(\mathbb{C}^n)$ has coordinates in an $\binom{n}{k}$ dimensional space, while the matrix of factors of Λ is in an $n \times k$ dimensional space. The polar coordinate method reduces the dimension of the space we are solving in by representing the exterior product by a "radius" and "angle", (γ, Ω), where $\gamma \in \mathbb{C}$ and $\Omega \in \mathbb{C}^{n \times k}$ is an orthonormal matrix spanning the factors of Λ.

Let $[\lambda_1 | \ldots | \lambda_k]$ be the matrix of factors of Λ, and let $\Omega = [\omega_1 | \ldots | \omega_k]$. Then for each

$j = 1, \ldots, k$ we have $\lambda_j = \Omega\alpha_j = \sum_{t=1}^{k} \alpha_{tj} w_t$, so that $[\lambda_1 | \ldots | \lambda_k] = \Omega\alpha$. Then

$$\begin{aligned} \Lambda &= \left(\sum_{t_1=1}^{k} \alpha_{1t_1} w_{t_1} \right) \wedge \ldots \wedge \left(\sum_{t_k=1}^{k} \alpha_{1t_k} w_{t_k} \right), && (2.8) \\ &= \sum_{t_1=1}^{k} \ldots \sum_{t_k=1}^{k} (\alpha_{1t_1} \cdots \alpha_{1t_k}) w_{t_1} \wedge \ldots \wedge w_{t_k}, && (2.9) \\ &= \sum_{(t_1,\ldots,t_k) \in P} (\alpha_{1t_1} \cdots \alpha_{1t_k}) w_{t_1} \wedge \ldots \wedge w_{t_k}, && (2.10) \end{aligned}$$

where P is the set of all permutations of $(1, \ldots, k)$. These last equalities follow since exterior products are multilinear and alternating.

Additionally, since exterior products are alternating we have

$$\begin{aligned} \Lambda &= \sum_{(t_1,\ldots,t_k) \in P} \operatorname{sgn}(t_1, \ldots, t_k)(\alpha_{1t_1} \cdots \alpha_{1t_k})\, w_1 \wedge \ldots \wedge w_k, && (2.11) \\ &= \det(\alpha)\, w_1 \wedge \ldots \wedge w_k. && (2.12) \end{aligned}$$

Let W^- be the unstable manifold of $A^-(\lambda)$ and W^+ the stable manifold of $A^+(\lambda)$. Then we can find $\alpha^{\pm}, \Omega^{\pm}$ such that

$$\begin{aligned} W^- &= \Omega^- \alpha^-,\ \det(\alpha^-) = \gamma^-, \\ W^+ &= \Omega^+ \alpha^+,\ \det(\alpha^+) = \gamma^+. \end{aligned}$$

Then the Evans function is

$$\begin{aligned} D(\lambda) &= \det(W_1^-, \ldots, W_k^-, W_{k+1}^+, \ldots W_n^+)\big|_{x=0}, \\ &= \gamma^+\gamma^- \det(\Omega^-, \Omega^+)\big|_{x=0}. \end{aligned}$$

2.2.1 Continuous orthogonalization. Suppose $W(x) = \Omega(x)\alpha(x)$ where $W(x), \Omega(x) \in \mathbb{C}^{n\times k}$ and Ω is orthonormal. Applying $W' = A(x,\lambda)W$, we obtain

$$\Omega'(x)\alpha(x) + \Omega(x)\alpha'(x) = A(x,\lambda)\Omega(x)\alpha(x).$$

By letting $B(x) = \alpha'\alpha^{-1}(x)$, we get the following system of equations for α, Ω:

$$\begin{aligned} \Omega'(x) &= A(x,\lambda)\Omega(x) - \Omega(x)B(x), \\ \alpha'(x) &= B(x)\alpha(x). \end{aligned} \tag{2.13}$$

We note that the dimension of this new system is greater than the original; thus we expect additional conditions on the ode to arise from the orthogonality condition $\Omega^*\Omega = I_{k\times k}$. Specifically, we have

$$\begin{aligned} 0 = I' = (\Omega^*\Omega)' &= (\Omega^*)'\Omega + \Omega^*\Omega', \\ &= (\Omega^*A^* - B^*\Omega^*)\Omega + \Omega^*(A\Omega - \Omega B), \\ &= \Omega^*(A^* + A)\Omega - B^*\Omega^*\Omega - \Omega^*\Omega B, \\ &= \Omega^*(A^* + A)\Omega - B^* - B. \end{aligned} \tag{2.14}$$

Thus $\Omega^*(A^* + A)\Omega - B^* - B = 0$ is a necessary condition for orthogonality. To see that this is sufficient when (2.13) is initialized with $\Omega_0^*\Omega_0 = I$, note that $(\Omega^*\Omega)' = 0$ implies that $\Omega^*\Omega$ is constant. Thus $\Omega^*(x)\Omega(x) = \Omega_0^*\Omega_0 = I_{k\times k}$.

We note that various choices of B have been used, notably in Drury's method ($B = \Omega^*A\Omega$) and Davey's method ($B = (\Omega^*\Omega)^{-1}\Omega^*A\Omega$). Drury's method can also be derived by setting $\Omega^*\Omega' = 0$, so that the change in Ω is orthogonal to the space spanned by Ω.

Substituting $B = \Omega^*A\Omega$ in (2.13), in polar coordinates our system becomes

$$\begin{aligned} \Omega' &= (I - \Omega\Omega^*)A\Omega, \\ \gamma' &= \operatorname{trace}(\Omega^* A\Omega)\gamma. \end{aligned} \tag{2.15}$$

2.3 The method of Kato

Suppose $P(\lambda)$ is an analytic projection. We would like to be able to find an analytically varying basis $R(\lambda)$ for the range of $P(\lambda)$. By standard linear ode theory, the initial value problem

$$\begin{aligned} R' &= P'R, \\ R(\lambda_0) &= R_0, \end{aligned} \tag{2.16}$$

has a unique solution that exists throughout the simply connected domain D. The solution $R(\lambda)$ of the (2.16) can then be found numerically.

Proposition 2.3. *The unique solution R of (2.16) satisfies*

(i) $PR = R$,

(ii) $PR' = 0$,

(iii) $R' = (P'P - PP')R$.

Proof.

(1)

$$\begin{aligned} (PR - R)' &= P'R + PR' - R', \\ &= P'R + PP'R - P'R, \\ &= PP'R - PP'PR, \\ &= -PP'(PR - R). \end{aligned}$$

Since $(PR - R)(\lambda_0) = P_0 R_0 - R_0 = 0$, by uniqueness of solutions $PR - R = 0$.

(2) $PR' = PP'R = PP'PR = 0$.

(3) $R' = P'R = P'PR = (P' - PP')R = (P'P - PP')R$. $\square$

Chapter 3. Rootfinding

3.1 Method of moments

3.1.1 Motivation. Suppose $f : G \to \mathbb{C}$ is analytic on a region $G \subset \mathbb{C}$ with roots $z_1, \ldots, z_n$. Then $g(z) = (z - z_1) \cdot \ldots \cdot (z - z_n)$ and $f(z)$ have the same roots in G. Note that

$$\begin{aligned} g(z) &= z^n - (z_1 + \ldots + z_n)z^{n-1} + \ldots + (-1)^n(z_1 \cdot \ldots \cdot z_n), \\ &= z^n - K_1 z^{n-1} + \ldots + (-1)^n K_n, \end{aligned}$$

where K_j is the jth order elementary symmetric polynomial in $z_1, \ldots, z_n$. By finding $K_1, \ldots K_n$, we can rootfind using $g(z)$, rather than a more difficult function $f(z)$.

3.1.2 Derivation of moments. Let $f : G \to \mathbb{C}$ by analytic in a region $G \subset \mathbb{C}$. Let Γ be a simple closed positively oriented contour in G with f nonzero on Γ. Let $z_1, \ldots, z_n$ be the n distinct roots of f in Γ, $c \in \mathbb{C}$ with $c \neq z_j \ \forall j$, and $p = 0, 1, 2, \ldots$. Then

$$M_p(f; c) := \frac{1}{2\pi i} \oint \frac{(z - c)^p f'(z)}{f(z)} \, dz = \sum_{j=1}^{n} m_j (z_j - c)^p \tag{3.1}$$

where m_j is the multiplicity of z_j.

Proof. We require only a brief generalization of the proof of the argument principle. Since f is analytic, for a zero z_j of f in Γ we have

$$f(z) = h(z)(z - z_j)^{m_j},$$

where h is analytic at z_j and $h(z_j) \neq 0$. Then in a neighborhood of z_j

$$\begin{aligned} g(z) = \frac{(z-c)^p f'(z)}{f(z)} &= \frac{(z-c)^p [h'(z)(z-z_j)^{m_j} + m_j h(z)(z-z_j)^{m_j-1}]}{h(z)(z-z_j)^{m_j}}, \\ &= \frac{(z-c)^p h'(z)}{h(z)} + \frac{m_j (z-c)^p}{z-z_j}. \end{aligned}$$

Since h is analytic and nonzero at z_j, we have $\mathrm{Res}(g; z_j) = m_j(z_j - c)^p$. Then Cauchy's residue theorem gives the result. □

We note that $M_0(0) = z_0^0 + \ldots + z_n^0 = n$ is the number of roots of f in Γ; similarly $\mu = M_1(0)/M_0(0)$ is the center of mass of the roots, while $M_2(\mu)/M_0(0)$ is their variance.

3.1.3 Using the moments of f. For an analytic function f, $M_0(0) = n$ may be used to determine the number of roots of f inside Γ. Then using Newton's formula, we can obtain constants $K_1, \ldots, K_n$ using the moments

$$\begin{aligned} M_1(0) &= z_1 + \ldots + z_n, && (3.2) \\ M_2(0) &= z_1^2 + \ldots + z_n^2, && (3.3) \\ &\vdots \\ M_n(0) &= z_1^n + \ldots + z_n^n. && (3.4) \end{aligned}$$

For example, when $M_0(0) = 2$ (f has two roots in Γ) then $M_1(0) = K_1$ and $M_2(0) = z_1^2 + z_2^2 = M_1(0)^2 - 2K_2$. Then $g(z) = (z - z_1)(z - z_2) = z^2 - K_1 z + K_2$, allowing us to easily solve for the roots of f.

We note that for $n > 4$ the roots $z_1, \ldots, z_n$ must be found numerically, since there is no closed form solution for the roots of $g(z)$. In practice polynomial rootfinding is ill-conditioned, so we typically use this method where n is small.

3.2 Computing the moments of f

3.2.1 Simpsons method. Using a degree two Lagrange interpolant through the points z_j, z_{j+1}, z_{j+2}, the integral of a function $g(z)$ may be approximated by

$$\int_{z_j}^{z_{j+2}} g(z)\,dz \approx a(z-z_{j+1})(z-z_{j+2}) + b(z-z_j)(z-z_{j+2}) + c(z-z_j)(z-z_{j+1})\,dz,$$

where a, b, and c are given by

$$\begin{aligned} a &= \frac{g(z_j)}{(z_j-z_{j+1})(z_j-z_{j+2})}, \\ b &= \frac{g(z_{j+1})}{(z_{j+1}-z_j)(z_{j+1}-z_{j+2})}, \\ c &= \frac{g(z_{j+2})}{(z_{j+2}-z_j)(z_{j+2}-z_{j+1})}. \end{aligned}$$

This may be further simplified to

$$\begin{aligned} \int_{z_j}^{z_{j+2}} g(z)\,dz \approx\ & \frac{z_{j+2}^3 - z_j^3}{3}(a+b+c) \\ & -\frac{z_{j+2}^3 - z_j^2}{2}\left(a(z_{j+1}+z_{j+2}) + b(z_j+z_{j+2}) + c(z_j+z_{j+1})\right) \\ & +(z_{j+2}-z_j)(az_{j+1}z_{j+2} + bz_jz_{j+2} + cz_jz_{j+1}). \end{aligned}$$

To compute $M_p(c)$ on a contour C, we let $g(z) = (z-c)^p f'(z)/f(z)$ where $f'(z)$ is approximated with some difference method (usually centered difference).

3.2.2 Application of the fast fourier transform. Let $\gamma(t) = z_0 + re^{2\pi it}, t \in [0,1]$. So γ is a simple closed positively oriented contour. Then $\gamma^{-1}(t) = \gamma(1-t) = z_0 + re^{2\pi i(1-t)} = z_0 + re^{-2\pi it}, t \in [0,1]$ and $\frac{d}{dt}\gamma^{-1}(t) = -2\pi rie^{-2\pi it}$. Then the pth moment of f about 0 with

respect to γ is given by

$$\begin{aligned}
M_p(0) &= \frac{1}{2\pi i}\oint_\gamma z^p \frac{f'(z)}{f(z)}dz = -\frac{1}{2\pi i}\oint_{\gamma^{-1}} z^p \frac{f'(z)}{f(z)}dz, \\
&= -\frac{1}{2\pi i}\int_0^1 (z_0 + re^{-2\pi it})^p \frac{f'\circ\gamma^{-1}}{f\circ\gamma^{-1}}(t)(-2\pi ri)e^{-2\pi it}dt, \\
&= r\int_0^1 \left(\sum_{k=0}^{p}\binom{p}{k} z_0^k (re^{-2\pi it})^{p-k}\right)\frac{f'\circ\gamma^{-1}}{f\circ\gamma^{-1}}(t)e^{-2\pi it}dt, \\
&= r^{p+1}\int_0^1 \left(\sum_{k=0}^{p}\binom{p}{k} (z_0/r)^k e^{-2\pi i(p-k)t}\right)\frac{f'\circ\gamma^{-1}}{f\circ\gamma^{-1}}(t)e^{-2\pi it}dt, \\
&= r^{p+1}\int_0^1 \left(\sum_{k=0}^{p}\binom{p}{k} (z_0/r)^k e^{-2\pi i(p-k+1)t}\right)\frac{f'\circ\gamma^{-1}}{f\circ\gamma^{-1}}(t)dt, \\
&= r^{p+1}\sum_{k=0}^{p}\binom{p}{k}(z_0/r)^k \left(\int_0^1 \frac{f'\circ\gamma^{-1}}{f\circ\gamma^{-1}}(t)e^{-2\pi i(p-k+1)t}dt\right).
\end{aligned}$$

Let x be a vector with

$$x(j) = \left(\frac{f'\circ\gamma^{-1}}{f\circ\gamma^{-1}}\right)\left(\frac{j-1}{2^N}\right), j = 1, \ldots, 2^N.$$

Then the left endpoint approximation of

$$\int_0^1 \frac{f'\circ\gamma^{-1}}{f\circ\gamma^{-1}}(t)e^{-2\pi i(p-k+1)t}dt$$

is

$$2^{-N}\sum_{j=1}^{2^N} x(j)e^{-2\pi i(p-k+1)(j-1)2^{-N}} = 2^{-N}X[p-k+2],$$

where X is the discrete fourier transform of x. Thus the left endpoint approximation of $M_p(0)$ is

$$r^{p+1}2^{-N}\sum_{k=0}^{p}\binom{p}{k}(z_0/r)^k X[p-k+2].$$

Also note that since γ is a close contour, the left endpoint, right endpoint, and trapezoidal approximations are the same.

3.2.3 Computing $M_0(0)$. Suppose f is an analytic function, and nonzero on a contour C. If $f(C)$ does not intersect the branch cut of $\log(z)$, then $\int_C \frac{f'(z)}{f(z)}dz = \log(f(z_1)) - \log(f(z_0))$ where z_0 is the initial point of C and z_1 the terminal point.

If $f(C)$ does pass through the branch cut of $\log(z)$, then $\int_C \frac{f'(z)}{f(z)}dz$ can be approximated by integrating over subcontours C_j where $f(C_j)$ does not intersect the branch cut of $\log(z)$. As the images $f(C_j)$ approach the branch cut, the sum of their integrals tends toward $\int_C \frac{f'(z)}{f(z)}dz$.

Since $\log(z) = \log|z| + i\arg(z)$, computing $\int_C \frac{f'(z)}{f(z)}dz$ is essentially a matter of determining how often, and with what orientation, $f(C)$ crosses the branch cut. For example, suppose $f(z) = (z-1+i)(z-1-i)$ and a contour C is given by $2e^{2\pi it}$, $t \in [0,1]$. Then $f(C)$ crosses the branch cut twice in the counterclockwise direction, so that $\int_C f'/f = 2\pi i + 2\pi i$, so that $M_0(0) = 2$; see Figure 3.1.

3.3 A bisection method

The algorithm for computing the winding number $W_0(0) = \int_C f'/f$ is more accurate and efficient than using integration. Once an eigenvalue's general location is known, a form of the bisection method can be used to get additional accuracy. Essentially $W_0(0)$ is computed for rectangular regions, which are further subdivided to obtain the required accuracy.

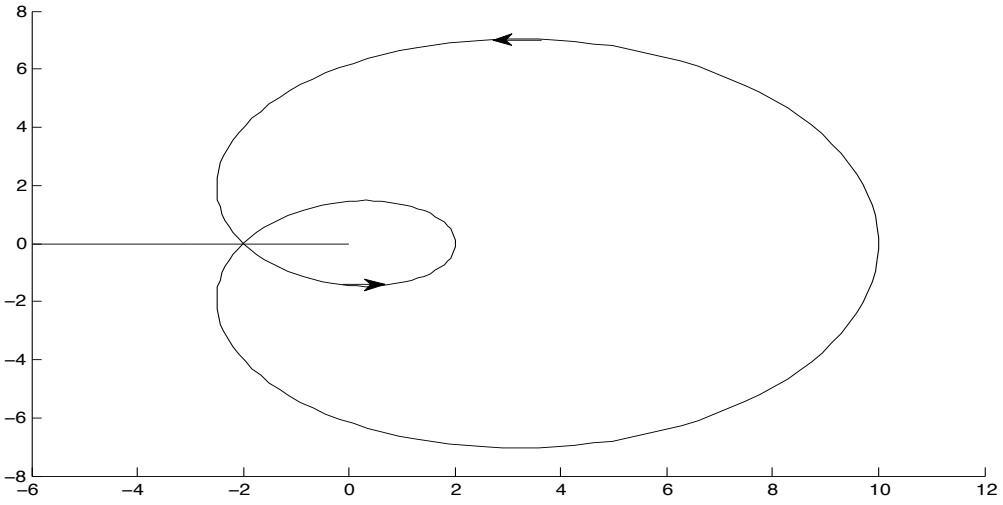

Figure 3.1: Example of a winding number calculation.

Chapter 4. Application: high Lewis number

4.1 The combustion model

We consider a model describing the combustion of a premixed fuel in one dimension. We assume that no heat is lost. In nondimensional coordinates the model is given by the equations.

$$\begin{aligned} u_t &= u_{xx} + y\Omega(u), \\ y_t &= \epsilon y_{xx} - \beta y\Omega(u), \end{aligned} \tag{4.1}$$

Here $u = u(x,t)$ is the scaled temperature and $y = y(x,t)$ is the concentration of the fuel.

This model describes a reaction which we assume begins at the ambient temperature, $u = 0$, with the reaction rate given by

$$\Omega(u) = \begin{cases} e^{-1/u} \text{ for } u > 0 \\ 0 \text{ otherwise.} \end{cases}$$

The parameter ϵ is the inverse Lewis number, representing the ratio of fuel diffusitivity to heat diffusitivity. The limiting case $\epsilon = 0$ characterizes combustion of solids, while an appropriate value of $\epsilon > 0$ characterizes gaseous combustion. The other parameter $\beta > 0$ represents the exothermicity of the system, the ratio of the activation energy to the heat of the reaction. In this chapter we will conduct a numerical study of the stability properties of traveling wave solutions of (4.1) as β varies.

We seek traveling wave solutions

$$\begin{aligned} u(x,t) &= \hat{u}(x-st), \\ y(x,t) &= \hat{y}(x-st), \end{aligned} \tag{4.2}$$

with wave speed $s > 0$ and asymptotically constant end states $(\hat{u}, \hat{y})(\pm\infty) = (u_\pm, y_\pm)$ where $(u_-, y_-) = (1/\beta, 0)$ and $(u_+, y_+) = (0, 1)$. We note that at $(u, y) = (0, 1)$ the fuel is at ambient temperature and has been untouched, while the state $(u, y) = (1/\beta, 0)$ describes the system with maximal heat and the fuel completely burned.

It has been shown that there is a unique wave speed $s > 0$ such that (4.1) has a nontrivial solution connecting the end-states exponentially. For $\epsilon = 0$ existence and uniqueness has been shown in [6, 29], and for $\epsilon \in (0, 1)$ in [2, 5, 20] . For $0 < \epsilon \ll 1$ existence and uniqueness has also been shown using geometric singular perturbation theory; see [19, 23, 8, 2, 10]. It is also known that the traveling wave $\hat{u}, \hat{y}$ satisfies $\hat{u}, \hat{y}, \hat{y}' > 0 > \hat{u}'$ for all x; see [24, 28, 22]. The wave profile has been numerically solved in [30]. See [9] for further background on this system.

4.2 Numerical solution of the wave profile

To find traveling waves $(\hat{u}, \hat{y})$ we make the coordinate change $(x, t) \to (x - st, t) = (\overline{x}, \overline{t})$ and look for steady state solutions of (dropping the bar notation)

$$\begin{aligned} u_t - su_x &= u_{xx} + y\Omega(u), \\ y_t - sy_x &= \epsilon y_{xx} - \beta y\Omega(u). \end{aligned} \tag{4.3}$$

Thus $\hat{u}$, $\hat{y}$ are solutions of the ordinary differential equations

$$\begin{aligned} u'' + su' + y\Omega(u) &= 0, \\ \epsilon y'' + sy' - \beta y\Omega(u) &= 0. \end{aligned} \tag{4.4}$$

We can write this as the first-order system

$$\begin{bmatrix} y_1 \\ y_2 \\ y_3 \\ y_4 \end{bmatrix}' = \begin{bmatrix} y_2 \\ -sy_2 - y_3\Omega(y_1) \\ y_4 \\ \frac{1}{\epsilon}(-sy_4 + \beta y_3\Omega(y_1)) \end{bmatrix}, \tag{4.5}$$

where $[y_1, y_2, y_3, y_4]^T = [u, u', y, y']^T$, and the new boundary conditions are

$$\begin{aligned} \begin{bmatrix} y_1 \\ y_2 \\ y_3 \\ y_4 \end{bmatrix}(-\infty) &= \begin{bmatrix} \frac{1}{\beta} \\ 0 \\ 0 \\ 0 \end{bmatrix}, \\ \begin{bmatrix} y_1 \\ y_2 \\ y_3 \\ y_4 \end{bmatrix}(+\infty) &= \begin{bmatrix} 0 \\ 0 \\ 1 \\ 0 \end{bmatrix}. \end{aligned} \tag{4.6}$$

Analyzing the Jacobian of the system at y_- reveals a one-dimensional unstable manifold, a one-dimensional stable manifold, and a two-dimensional centered manifold. We are looking for solutions with exponential decay; thus we obtain a total of three projective conditions at $x = -\infty$. Similarly, at y_+ there is a two-dimensional unstable manifold and a two-dimensional centered manifold, giving two projective conditions at $x = \infty$. We also require a phase condition at $x = 0$. Since the number of conditions must equal the dimension of the

ode, we look for further simplify the system.

4.2.1 Reducing the dimension of the system. Consider again the ode (4.4). Multiplying the first equation by β and adding the second equation, we get

$$\beta u'' + \beta s u' + \epsilon y'' + s y' = 0. \tag{4.7}$$

Integrating from $-\infty$ to x, we get the conserved quantity

$$\begin{aligned} \beta u' + \beta s(u - u_-) + \epsilon y' + s(y - y_-) &= 0, \\ \beta u' + \beta s(u - 1/\beta) + \epsilon y' + s(y - 0) &= 0, \\ \beta u' + \beta s u + \epsilon y' + s y &= s. \end{aligned} \tag{4.8}$$

Note that our conserved quantity can be expressed as

$$y_3 = \frac{1}{s}\left[s - \beta s y_1 - \beta y_2 - \epsilon y_4\right]. \tag{4.9}$$

Let $z_1 = y_1, z_2 = y_2, z_3 = y_4$. Then we get

$$\begin{bmatrix} z_1 \\ z_2 \\ y_3 \end{bmatrix}' = \begin{bmatrix} z_2 \\ -s z_2 - \frac{1}{s}\left[s - \beta s z_1 - \beta z_2 - \epsilon z_3\right]\Omega(z_1) \\ \frac{1}{\epsilon}(-s z_3 + \frac{\beta}{s}\left[s - \beta s z_1 - \beta z_2 - \epsilon z_3\right]\Omega(z_1)) \end{bmatrix}, \tag{4.10}$$

with

$$\begin{aligned}\begin{bmatrix} z_1 \\ z_2 \\ z_3 \end{bmatrix}(-\infty) &= \begin{bmatrix} 1/\beta \\ 0 \\ 0 \end{bmatrix}, \\ \begin{bmatrix} z_1 \\ z_2 \\ z_3 \end{bmatrix}(+\infty) &= \begin{bmatrix} 0 \\ 0 \\ 0 \end{bmatrix}.\end{aligned} \tag{4.11}$$

We write this as $z' = F(z)$.

4.2.2 Finding the projective conditions. For $x = \pm\infty$, we can simplify dF to

$$dF(z) = \begin{pmatrix} 0 & 1 & 0 \\ \beta\Omega(z_1) & -s + \beta\Omega(z_1)/s & \epsilon\Omega(z_1)/s \\ -\beta^2\Omega(z_1)/\epsilon & -\beta^2\Omega(z_1)/(\epsilon s) & -s/\epsilon - \beta\Omega(z_1)/s \end{pmatrix}, \tag{4.12}$$

and we get

$$dF_- = \begin{pmatrix} 0 & 1 & 0 \\ \beta e^{-\beta} & -s + \beta e^{-\beta}/s & \epsilon e^{-\beta}/s \\ -\beta^2 e^{-\beta}/\epsilon & -\beta^2 e^{-\beta}/(\epsilon s) & -s/\epsilon - \beta e^{-\beta}/s \end{pmatrix}, \tag{4.13}$$

$$dF_+ = \begin{pmatrix} 0 & 1 & 0 \\ 0 & -s & 0 \\ 0 & 0 & -s/\epsilon \end{pmatrix}. \tag{4.14}$$

For this new system $z' = F(z)$, at z_- there is a one-dimensional unstable manifold and a

two-dimensional stable manifold, giving two projective conditions at $x = -\infty$. At z_+ there is a one-dimensional centered manifold and a two-dimensional stable manifold, giving two projective conditions at $x = +\infty$. We then add a phase condition to determine a unique solution for the system. We then double the dimension of the system to solve on the domain $[0, \infty)$, and add three matching conditions. Since the wave speed $s > 0$ is unknown, we add a constant variable to our system to solve for s. This gives us a seven-dimensional system with seven boundary conditions.

This gives us two projective conditions at $-\infty$ and one projective condition at $+\infty$, giving a total of three projective conditions. Note that there are three matching conditions, and one phase condition, for a total of seven boundary conditions.

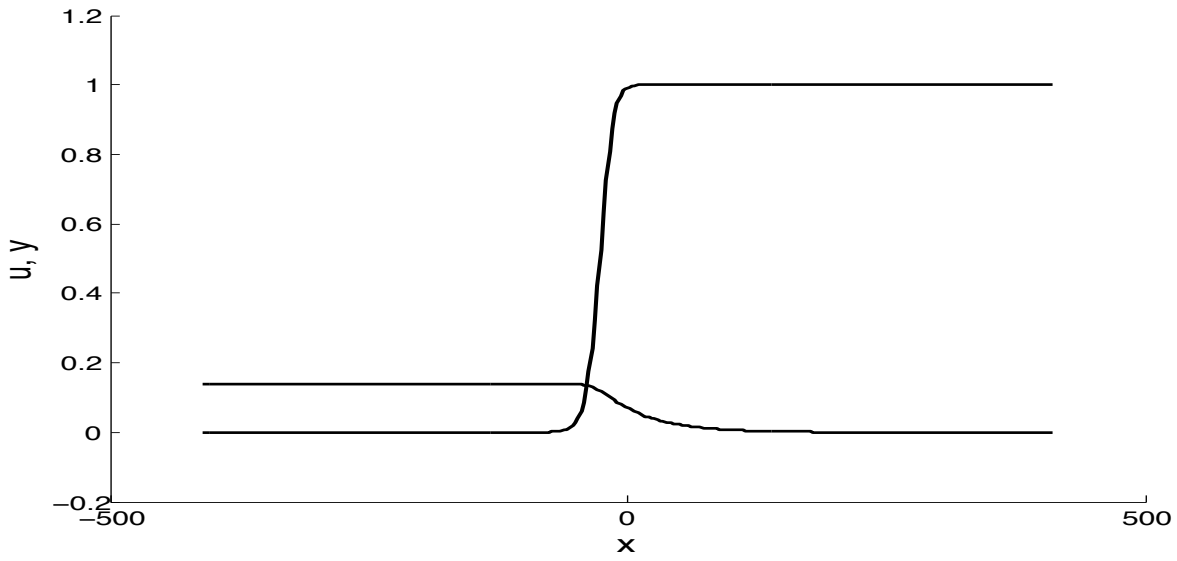

Figure 4.1: Traveling wave solutions $\hat{u}$ and $\hat{y}$. Note that $\hat{u}'(x) < 0$ and $\hat{y}'(x) > 0$ for all x.

4.3 Evans function computation

In this section we use the Evans function study the unstable eigenvalues of L. The Evans function $D(\lambda)$ is analytic to the right of the essential spectrum and is defined as the Wronskian of decaying solutions of the eigenvalue equation for the linearized operator. While the

Evans function is generally too complex to compute explicitly, it can readily be computed numerically, even for large systems.

Since the Evans function is analytic in the right-half plane, we can numerically compute the winding number there. This method allows us to systematically detect the roots of $D(\lambda) = 0$ within (and hence the eigenvalues of our system). As a result, we can produce bifurcation diagrams observing the onset of instability. This was done first by Evans and Feroe and has since been applied to other systems.

It has been shown analytically [11] that for $\tau \sim O(1)$ and $\beta \gg 1$, a Hopf bifurcation occurs with two complex eigenvalues traveling into the right-half plane. For $\tau = .1$ the Evans function was used to analyze the spectrum of L. Numerically, as β was increased the wave front was seen to move from stability to instability at $\beta = 7.026$.

We begin by writing the eigenvalue problem as a first-order system $W' = A(x, \lambda)W$, where

$$A(x,\lambda) = \begin{pmatrix} 0 & 1 & 0 & 0 \\ \lambda + \hat{y}\hat{u}^{-2}e^{-1/\hat{u}} & -s & -e^{-1/\hat{u}} & 0 \\ 0 & 0 & 0 & 1 \\ \frac{\beta}{\varepsilon}\hat{v}\hat{u}^{-2}e^{-1/\hat{u}} & 0 & \frac{1}{\varepsilon}(\lambda + \beta e^{-1/\hat{u}}) & -\frac{s}{\varepsilon} \end{pmatrix}, \quad W = \begin{pmatrix} p_1 \\ q_1 \\ p_2 \\ q_2 \end{pmatrix}, \quad ' = \frac{d}{dx},$$

and $\Omega_{\hat{u}}(\hat{u}) = e^{-1/\hat{u}}/\hat{u}^2$. We note that eigenvalues correspond to nontrivial solutions $W(x)$ satisfying the boundary conditions $W(\pm\infty) = 0$. We also note that $A(x, \lambda)$ is asymptotically constant in x, since $\hat{u}$ is. Thus at each end-state, $W(x)$ must satisfy the constant-coefficient system

$$W' = A_{\pm}(\lambda)W.$$

Solutions satisfying the boundary condition $W(\pm\infty) = 0$ must arise from the unstable manifold $W_1^- \wedge W_2^-$ at $x = -\infty$ and the stable manifold $W_3^+ \wedge W_4^+$ at $x = \infty$. Thus, eigenvalues of L correspond to values of λ where these manifolds intersect, the manifolds

intersecting exactly when $D(\lambda) := \det(W_1^- W_2^- W_3^+ W_4^+)_{|x=0}$ is zero.

The unstable/stable modes of $W_1^- \wedge W_2^-$ and $W_3^+ \wedge W_4^+$ can cause numerical instabilities in the shooting scheme. It has been shown that by rescaling W and shooting in centered coordinates, good numerical results can be obtained. To rescale W, we let $W(x) = e^{\mu^- x} V(x)$ where μ^- is the growth mode associated with $W_1^- \wedge W_2^-$. We then integrate using the ode $V'(x) = (A(x,\lambda) - \mu^- I)V(x)$. We rescale W similarly at $x = +\infty$.

To ensure analytically varying Evans function output, the initial data $V(-L)$ and $\tilde{V}(L)$ must be chosen analytically. Instead of using eigenvectors as a basis for the unstable/stable manifolds, the method of Kato allows us to find analytically varying spectral projectors.

4.4 Rootfinding for $D(\lambda)$

Rootfinding for the Evans function was done using the method of moments. Generally, for a function f analytic inside and on a simple closed positively oriented curve Γ, if f is nonzero on Γ and $z_1, \ldots, z_n$ are the roots of $f(z)$ inside Γ, then the p^{th} moment of f about z^* is given by

$$M_p(z^*) = \frac{1}{2\pi i} \oint \frac{(z - z^*)^p f'(z)}{f(z)} = \sum_{k=1}^{n} (z_k - z^*)^p.$$

Specifically, $M_0(0)$ gives the number of roots inside Γ while $M_1(0)$ gives the sum of roots. For $\tau = .1$, $\beta = 7.026$, two eigenvalues cross the imaginary axis into the right half-plane at $\pm 6.8i \times 10^{-4}$. Since $D(\lambda)$ is analytic in the right half-plane, the eigenvalues were tracked using the method of moments. By taking successive small circular contours about the individual eigenvalues and regulating the relative error in the output, approximating $M_1(0)$ with simpsons rule gives a reasonable estimation of the eigenvalues. At $\beta = 10.232$ the eigenvalues combine to form an eigenvalue of multiplicity two on the real axis, then split along the reals. They then travel toward the origin along the real line.

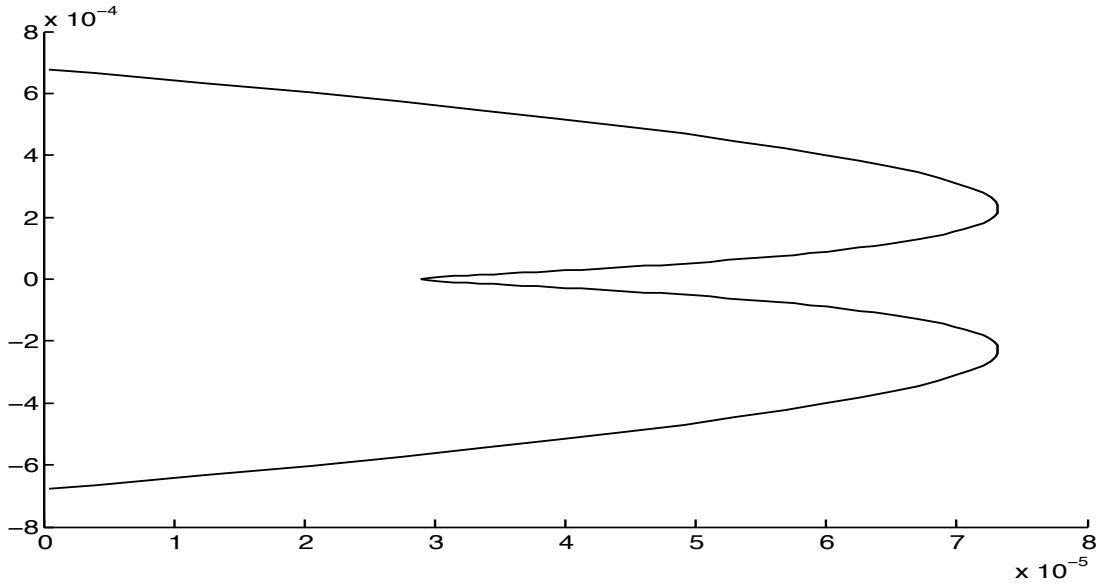

Figure 4.2: The path of the eigenvalues $\lambda_{\pm}$ in the complex plane, crossing the imaginary axis at $\beta = 7.026$ and joining on the real axis when $\beta = 10.232$.

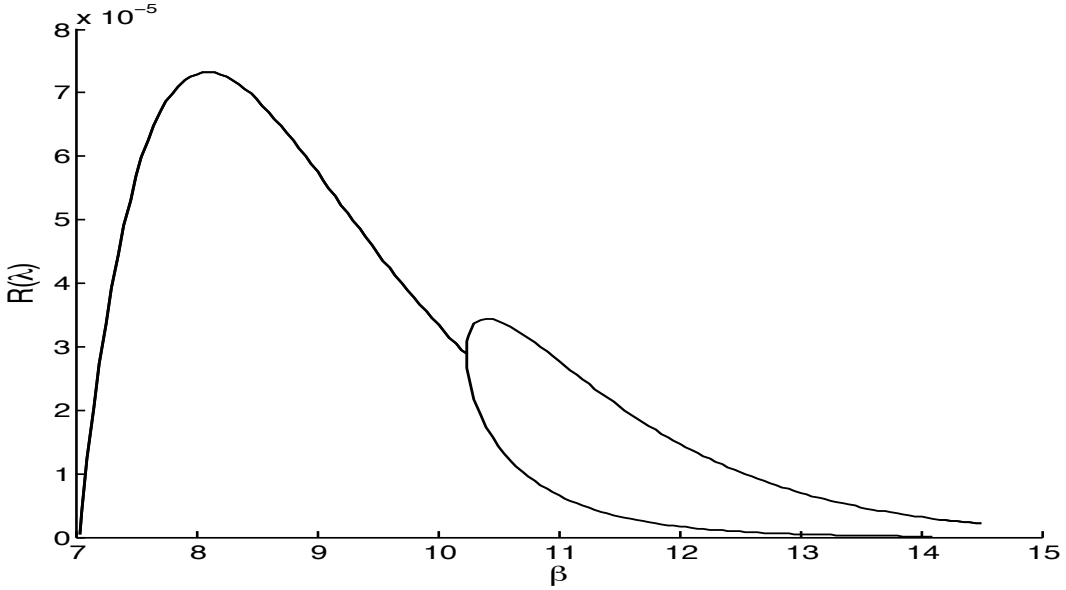

Figure 4.3: Real part of the eigenvalues for $\beta \in [7.026, 14.1]$.

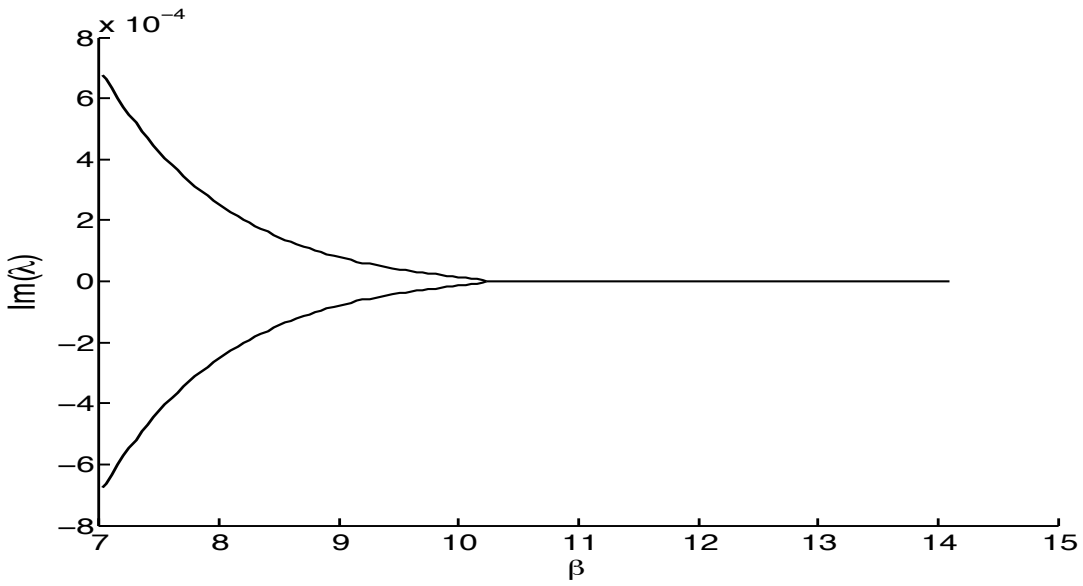

Figure 4.4: Imaginary part of the eigenvalues for $\beta \in [7.026, 14.1]$.

Bibliography

[1] J. Alexander, R. Gardner, and C. Jones, *A topological invariant arising in the stability analysis of travelling waves*, J. Reine Angew. Math., 410 (1990), pp. 167–212.

[2] S. Balasuriya, G. Gottwald, J. Hornibrook, and S. Lafortune, *High Lewis number combustion wavefronts: a perturbative Melnikov analysis*, SIAM J. Appl. Math., 67 (2006/07), pp. 464–486 (electronic).

[3] B. Barker, *Evans function computation.*, Master's thesis, Brigham Young University, Provo, 2009.

[4] B. Barker, J. Humpherys, K. Rudd, and K. Zumbrun, *Stability of viscous shocks in isentropic gas dynamics*, Comm. Math. Phys., 281 (2008), pp. 231–249.

[5] H. Berestycki, B. Nicolaenko, and B. Scheurer, *Traveling wave solutions to combustion models and their singular limits*, SIAM J. Math. Anal., 16 (1985), pp. 1207–1242.

[6] J. Billingham, *Phase plane analysis of one-dimensional reaction diffusion waves with degenerate reaction terms*, Dyn. Stab. Syst., 15 (2000), pp. 23–33.

[7] R. W. R. Darling, *Differential forms and connections*, Cambridge University Press, Cambridge, 1994.

[8] N. Fenichel, *Geometric singular perturbation theory for ordinary differential equations*, J. Differential Equations, 31 (1979), pp. 53–98.

[9] A. Ghazaryan, J. Humpherys, and J. Lytle, *Spectral instability in high lewis number combustion fronts*. Preprint, 2011.

[10] A. Ghazaryan and C. Jones, *On the existence of high lewis number combustion fronts*, Mathematics and Computers in Simulation, In Press, Corrected Proof (2010), pp. –.

[11] V. Gubernov, G. N. Mercer, H. S. Sidhu, and R. O. Weber, *Evans function stability of combustion waves*, SIAM J. Appl. Math., 63 (2003), pp. 1259–1275 (electronic).

[12] N. Hale and D. R. Moore, *A sixth-order extension to the matlab package bvp4c of j. kierzenka and l. shampine*, Tech. Rep. NA-08/04, Oxford University Computing Laboratory, May 2008.

[13] D. Henry, *Geometric theory of semilinear parabolic equations*, vol. 840 of Lecture Notes in Mathematics, Springer-Verlag, Berlin, 1981.

[14] P. Howard and K. Zumbrun, *Pointwise estimates and stability for dispersive-diffusive shock waves*, Arch. Ration. Mech. Anal., 155 (2000), pp. 85–169.

[15] J. Humpherys, *On the shock wave spectrum for isentropic gas dynamics with capillarity*, J. Differential Equations, 246 (2009), pp. 2938–2957.

[16] J. Humpherys, O. Lafitte, and K. Zumbrun, *Stability of isentropic Navier-Stokes shocks in the high-Mach number limit*, Comm. Math. Phys., 293 (2010), pp. 1–36.

[17] J. Humpherys and K. Zumbrun, *An efficient shooting algorithm for Evans function calculations in large systems*, Phys. D, 220 (2006), pp. 116–126.

[18] J. C. Humpherys, *Spectral energy methods and the stability of shock waves*, ProQuest LLC, Ann Arbor, MI, 2002. Thesis (Ph.D.)–Indiana University.

[19] C. K. R. T. Jones, *Geometric singular perturbation theory*, in Dynamical systems (Montecatini Terme, 1994), vol. 1609 of Lecture Notes in Math., Springer, Berlin, 1995, pp. 44–118.

[20] Y. I. Kanel, *On steady state solutions to systems of equations arising in combustion theory*, Dokl. Akad. Nauk SSSR, 149 (1963), pp. 367–369.

[21] T. Kato, *Perturbation theory for linear operators*, Classics in Mathematics, Springer-Verlag, Berlin, 1995. Reprint of the 1980 edition.

[22] E. Logak, *Mathematical analysis of a condensed phase combustion model without ignition temperature*, Nonlinear Anal., 28 (1997), pp. 1–38.

[23] E. Logak and V. Loubeau, *Travelling wave solutions to a condensed phase combustion model*, Asymptotic Anal., 12 (1996), pp. 259–294.

[24] M. Marion, *Qualitative properties of a nonlinear system for laminar flames without ignition temperature*, Nonlinear Anal., 9 (1985), pp. 1269–1292.

[25] C. Mascia and K. Zumbrun, *Pointwise Green's function bounds and stability of relaxation shocks*, Indiana Univ. Math. J., 51 (2002), pp. 773–904.

[26] ——, *Pointwise Green function bounds for shock profiles of systems with real viscosity*, Arch. Ration. Mech. Anal., 169 (2003), pp. 177–263.

[27] D. H. Sattinger, *On the stability of waves of nonlinear parabolic systems*, Advances in Math., 22 (1976), pp. 312–355.

[28] P. Simon, J. Merkin, and S. Scott, *Bifurcations in non-adiabatic flame propagation models*, Focus on Combustion Research, Nova Science Publishers, New York, 2006.

[29] F. Varas and J. M. Vega, *Linear stability of a plane front in solid combustion at large heat of reaction*, SIAM J. Appl. Math., 62 (2002), pp. 1810–1822 (electronic).

[30] R. O. Weber, G. N. Mercer, H. S. Sidhu, and B. F. Gray, *Combustion waves for gases* (Le = 1) *and solids* (Le $\to \infty$), Proc. Roy. Soc. London Ser. A, 453 (1997), pp. 1105–1118.

[31] K. Zumbrun, *Numerical error analysis for evans function computations: a numerical gap lemma, centered-coordinate methods, and the unreasonable effectiveness of continuous orthogonalization.* Preprint, 2009.

[32] K. Zumbrun and P. Howard, *Pointwise semigroup methods and stability of viscous shock waves*, Indiana Univ. Math. J., 47 (1998), pp. 741–871.